John von Neumann Institute for Computing

Electrical Conduction in Molecular Junctions

P. Stampfuß, J. Heurich, M. Wegewijs, M. Hettler,
J. C. Cuevas, H. Schoeller, W. Wenzel, G. Schön

published in

NIC Symposium 2004, Proceedings,
Dietrich Wolf, Gernot Münster, Manfred Kremer (Editors),
John von Neumann Institute for Computing, Jülich,
NIC Series, Vol. **20**, ISBN 3-00-012372-5, pp. 101-114, 2003.

http://www.fz-juelich.de/nic-series/volume20

Electrical Conduction in Molecular Junctions

P. Stampfuß[1], J. Heurich[2], M. Wegewijs[3], M. Hettler[1], J. C. Cuevas[2], H. Schoeller[3], W. Wenzel[3], and G. Schön

[1] Institut für Nanotechnologie, Forschungszentrum Karlsruhe
Postfach 3640, 76021 Karlsruhe, Germany
E-mail: {*stampfuss, hettler, wenzel*}*@int.fzk.de*

[2] Institut für Theoretische Festkörperphysik, Universität Karlsruhe
76128 Karlsruhe, Germany
E-mail: {*heurich,cuevas,schoen*}*@tkm.uni-karlsruhe.de*

[3] Theoretische Physik A, RWTH Aachen, 52074 Aachen, Germany
E-mail: {*wegewijs,schoeller*}*@physik.rwth-aachen.de*

Much experimental effort has been devoted in recent years to measure the electrical current through single molecule in covalent contact with metallic electodes. We briefly review the theoretical models to calculate the current through such molecular junctions in the limit of strong and weak coupling of the molecule to the electrodes. For strong coupling we discuss the current-voltage characteristic of organic molecules and of the recently measured hydrogen molecule. For weak coupling we investigate electronic transport through benzene and elucidate the mechanism for the total collapse of the current in a finite voltage window.

1 Introduction

The continuous miniaturization of electronic devices may ultimately require the use of single molecules or atoms as electronically active elements in a variety of applications[1,2]. Advances in the manipulation of single molecules in recent years have made it possible measure the current through an individual molecule contacted between two electrodes (see Fig. 1)[3–8]. Interesting and novel effects, such as negative differential conductance[9], were observed in some of these experiments, but many of these remain unexplained. In addition to generic principles of nanoscale physics, e.g. Coulomb blockade[6,10,11], the chemistry and geometry of the molecular junction emerge as the fundamental tunable characteristics of molecular junctions[3,4,12–16].

When the molecule is coupled *weakly* to the electrodes, i.e. via electron tunneling, charging effects, semi-classically determined by the small capacitance of the molecule, become important. The interplay of charging effects with the specific structure of the molecular orbitals leads to nontrivial current voltage ($I-V$) characteristics[9,17,18]. Very recent experiments demonstrated both Coulomb blockade and the Kondo effect in three terminal transport through a single molecular level[19,20].

When the molecule is coupled *strongly* to the electrodes, the electron transport is ballistic. The hybridization between molecular and electrode orbitals leads to a broading of the former, which can lead to interesting effects in the current-voltage characteristic . In the following we summarize our investigations of these two theoretically accessible limits. We present an atomistic theory that bridges traditional concepts of mesoscopic and molecular physics to describe transport through single organic molecules in qualitative agreement with recent break-junction experiments[21]. We show how the specific properties of

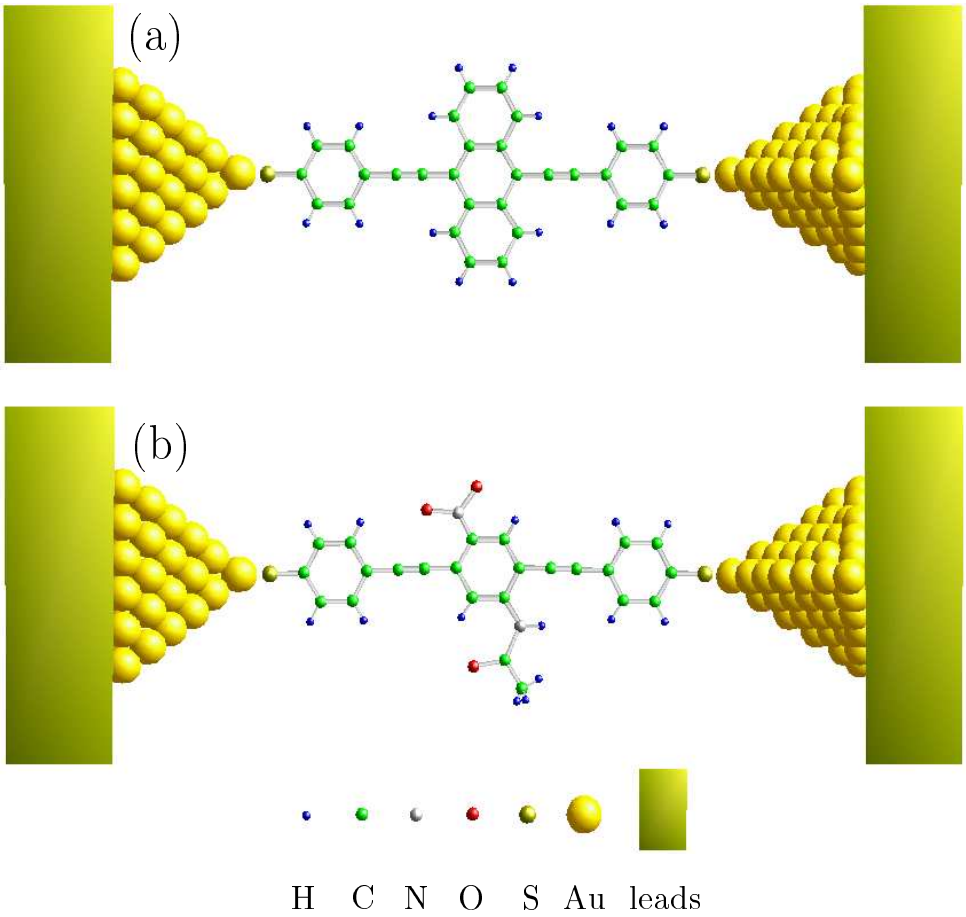

Figure 1. Scheme of the single-molecule contacts analyzed in this work. The two organic molecules attached to gold electrodes, which were experimentally investigated in Ref. 8, are referred to as: (a) “symmetric molecule”, and (b) “asymmetric molecule”.

individual MOs are reflected in their contribution to the current. Secondly we investigate conduction through the hydrogen molecule[22] in order to explain a recent break-junction experiment[23].

In the *weak-coupling* limit we present a theoretical model that predicts strong negative differential conductance in tunneling transport through benzene[18] and elucidate the physical mechanism responsible for this effect.

2 Ballistic Transport

2.1 Model

We calculate the current through a single molecule attached to metallic electrodes using Landauer transport theory in analogy to the analysis of transport in atomic-size contacts[24]. Since the conductance is mainly determined by the narrowest part of the junction, only the electronic structure of this “central cluster” must be resolved in detail. It is therefore

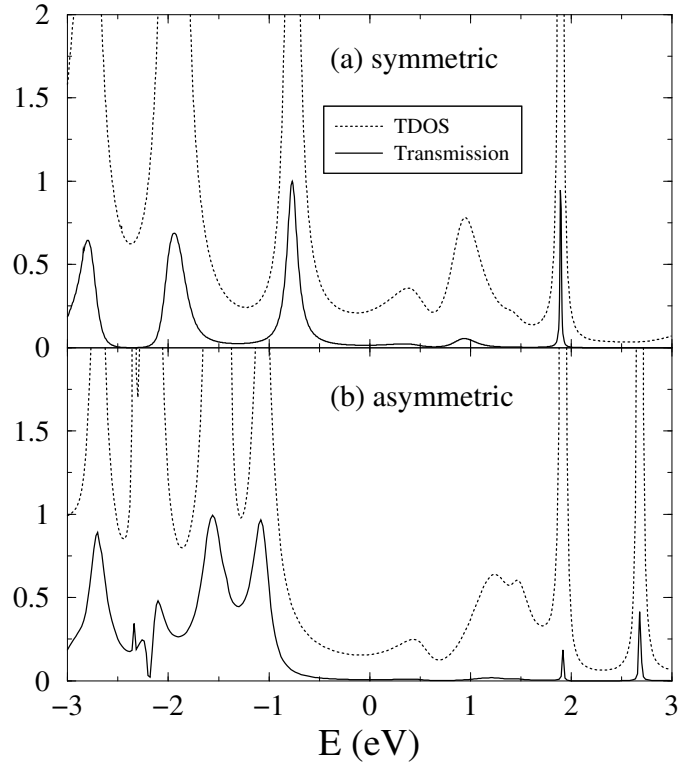

Figure 2. Total density of states (TDOS) of the molecule and zero-bias total transmission as a function of the energy for both molecules. The Fermi energy is set to zero (see[21]).

sensible to decompose the overall Hamiltonian of the molecular junction as

$$\hat{H} = \hat{H}_L + \hat{H}_R + \hat{H}_C + \hat{V}, \tag{1}$$

where $\hat{H}_C$ describes the "central cluster" of the system, $\hat{H}_{L,R}$ describe the left and right electrode respectively, and $\hat{V}$ gives the coupling between the electrodes and the central cluster (see Figure (1)).

The electronic structure of the "central cluster" is calculated with density functional (DFT) methods, while the left and right reservoirs are modeled as two perfect semi-infinite crystals of the corresponding metal using a tight-binding parameterization[25]. $\hat{V}$ is the coupling matrix element that describes the coupling between the leads and the central cluster. The "central cluster" is not necessarily confined to the molecule, but may, in principle, contain arbitrary parts of the metallic electrode. The inclusion of part of the leads in the *ab initio* calculation was shown to improve the description of the molecule-leads coupling[14], in particular regarding charge transfer between the molecule and the electrodes. The Fermi energy of the overall system is determined by the charge neutrality condition of the central cluster.

In order to obtain the current for a constant bias voltage, V, between the leads, we

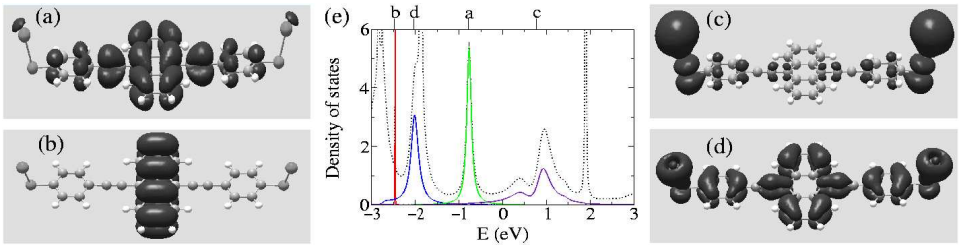

Figure 3. (a-d) Charge-density plots of four molecular orbitals of the central cluster for the symmetric molecule. Panel (a) displays the HOMO and (c) the LUMO, which is twofold degenerate. (b) shows a confined orbital that contributes little to the current, while the MO in (d) is almost as important as the LUMO despite its difference in energy. Panel (e) shows the total density of states of the central cluster (dotted line) and the individual contributions of the four molecular orbitals (color lines). The level positions are indicated on top of this panel. The contributions of the different MOs to the conduction channel at the Fermi energy (set to zero) are: $|\alpha_a|^2 = 0.007$, $|\alpha_b|^2 = 10^{-11}$, $|\alpha_c|^2 = 0.06$, $|\alpha_d|^2 = 0.02$ (see[21]).

make use of non-equilibrium Green function techniques. Since the Hamiltonian of Eq. (1) does not contain inelastic interactions, the current follows from the Landauer formula[26]:

$$I = \frac{2e}{h} \int_{-\infty}^{\infty} d\epsilon \, \mathrm{Tr} \left\{ \hat{t}\hat{t}^{\dagger} \right\} \left[f(\epsilon - eV/2) - f(\epsilon + eV/2) \right], \tag{2}$$

where f is the Fermi function and $\hat{t}$ is the energy and voltage dependent transmission matrix. The details of the formalism and of the calculation are reported in Ref. 21.

The understanding of the mechanism of electronic transport is aided the definition of *conduction channels* as eigenfunctions of $\hat{t}\hat{t}^{\dagger}$. Such an analysis allows to quantify the contribution to the transport of *every individual molecular level*. The channels arise as a linear combination of the molecular orbitals $|\phi_j\rangle$ of the central cluster, i.e. $|c\rangle = \sum_j \alpha_{cj} |\phi_j\rangle$, and the corresponding eigenvalues determine their contribution to the conductance.

2.2 Results

In the following we briefly review the methodology to analyze the current through organic molecules, in the context of the molecules shown in Figure (1)[8,21]. We then summarize our results for electronic transport through hydrogen, one of the prototypical test systems.

Experimentally, both molecules were contacted several times and the nature of the I-V characteristics was found to vary with the quality of the contact. For this reason, theory can presently aim to elucidate important reproducible features of the experiment under the assumption that the contact to the electrodes is well defined. Since there is no direct experimental information regarding the geometry of the molecule and its attachment to the leads, the overall geometry of the central cluster was relaxed without additional constraints in our calculations, resulting in the Au atom being out of the molecular plane.

We start by analyzing the linear response regime: Figure (2) shows the total density of states (TDOS) of the molecule and the zero-bias total transmission as a function of energy. As can be seen in the TDOS, in the covalent bond between Au and S results in a strong hybridization between the molecular orbitals and the extended states of the metallic

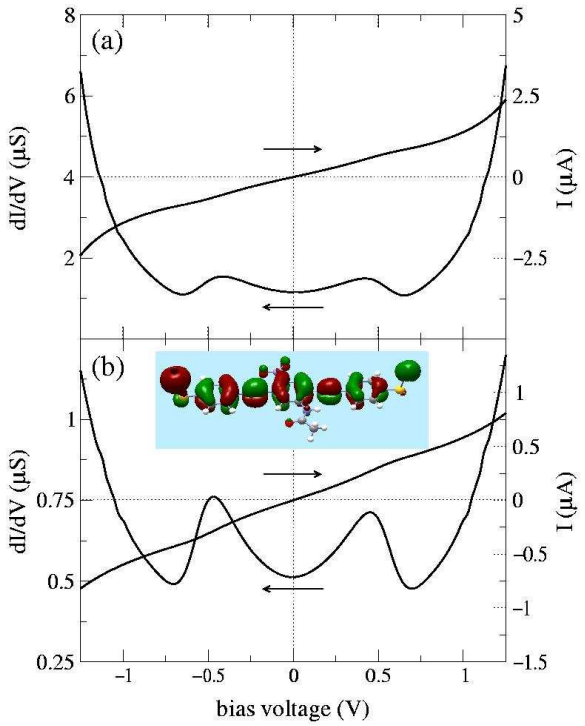

Figure 4. I-V characteristics and differential conductance for the symmetric (a) and asymmetric (b) molecules (see[21]). The inset in (b) shows the charge-density plot of the HOMO for the asymmetric molecule. Notice the intrinsic asymmetry of the charge distribution in the gold atoms.

electrodes. The formation of wide energy bands suggests the absence of Coulomb blockade in this type of molecular junctions.

The zero-bias total transmission as a function of energy follows closely the TDOS. The transmission is dominated overwhelmingly by a single channel in the energy window shown in Fig. 2, and the corresponding eigenvalues of $\hat{t}\hat{t}^{\dagger}$ at the Fermi energy are $T_{sym} = 0.014$ and $T_{asym} = 0.006$. The decomposition of this channel into molecular orbitals provides us information on the relevance of the different molecular levels. Figure (3) (a)-(d) show charge-density plots for some representative MOs and (e) shows their individual contribution to the TDOS. Figure (3)(a) indicates that the highest occupied molecular orbital (HOMO) is confined to the interior of the molecule and its weight at the gold atoms is rather small. Consequently, in spite of its privileged energy position, the HOMO does not give a significant contribution to the current. The lowest unoccupied molecular orbital (LUMO), see Figure (3)(c), exhibits the opposite behavior, i.e. it is very well coupled to the leads through the $6s$ atomic orbital of the gold atoms (notice that it has a width of about 4 eV in the density of states), but the charge is mainly localized on the Au and S atoms. The interplay of these two factors yields a contribution of $\approx 6\%$ of the total current. Figure (3)(b,d) shows two further MOs with similar energy but very different contribution to the channel. While the localized MO (b) carries almost no current, the extended

and well coupled MO (d) has significant weight. Consequently there are three ingredients which determine the contribution of a MO to the current: (i) its energy position (distance to the Fermi energy), (ii) its bridging extent (whether it is extended or localized), and (iii) its coupling to the leads. Our analysis provides a counterexample to the conventional wisdom that the HOMO and the LUMO dominate the transport properties.

Figure (4) shows the I-V curves for both molecules in the experimental voltage range. Both the order of magnitude and shape of the current and conductance agree qualitatively with the experimental results. There is no pronounced voltage dependence of the transmission due to the smooth density of states of the gold electrodes in the energy region explored here. The non-linearities in these I-V curves can be then understood by a simple inspection of the energy dependence of the zero-bias transmission. For instance, the pronounced increase in the conductance around 1 V is due to the fact that we approach the resonant condition for the HOMO and LUMO. The current-voltage characteristic in the figure were computes using the zero-field molecular spectra. At a finite bias one should in principle determine how the voltage modifies the molecular spectra, which in turn control the current. We performed DFT calculations at a fixed electric field and found no significant differences in the transmission in the voltage range explored in the experiments.

In agreement with the experiment, the I-V of the symmetric molecule is symmetric with respect to voltage inversion, while the one of the asymmetric molecule is asymmetric. The asymmetry of the I-V curve arises from the left/right asymmetry of the scattering rates. This asymmetry can be due to an asymmetry of either the leads or of the coupling of the leads to the molecule. The latter is influenced by intrinsic properties of the molecule, such as the charge distribution of the contributing MOs is asymmetric (see inset Figure (4)(b)). In the case of the symmetric molecule, we were able to induce asymmetries into the I-V characteristic by distorting the geometry of one of the lead fragments in the central cluster. This fact was nicely demonstrated in the experiment (see Fig. 5 in Ref. 8). We investigated several other scenarios regarding the number of gold atoms, their geometry and the coupling and found predictable variations of the I-V's with theses changes.

The measurement of the conductance of an *individual hydrogen molecule*[23,22] provides a valuable opportunity to analyze the emerging concepts on the electrical conduction in single-molecule devices in the perhaps simplest possible system. In contrast to results for organic molecules described above, molecular hydrogen has a conductance close to one quantum unit, carried by a single channel. This result belies the conventional wisdom because the closed-shell configuration of H_2 results in a huge gap between its bonding and antibonding states, making it a perfect candidate for an insulating molecule.

In order to investigate the transport through the hydrogen bridge we have performed DFT calculations of the linear conductance using the method described above[21].The most probable configuration is shown in the inset of Figure (5), where the H_2 is coupled to a single Pt atom on either side (top position). In this geometry the vibrational mode of the center of mass motion of H_2, has an energy of 55.6 meV comparable with the experimental values. In Figure (5) we show the transmission and the LDOS projected into the orbitals of one of the H atoms. The total transmission at the Fermi energy is $T_{tot} = 0.86$ and it is largely dominated by a single channel, in agreement with experimental results.

In principle there are other geometries compatible with the vibrational modes analysis. However, based on the channel analysis performed in the experiment many geometries can be ruled out. As an example we consider the situation sketched in the inset of Fig. 6 where

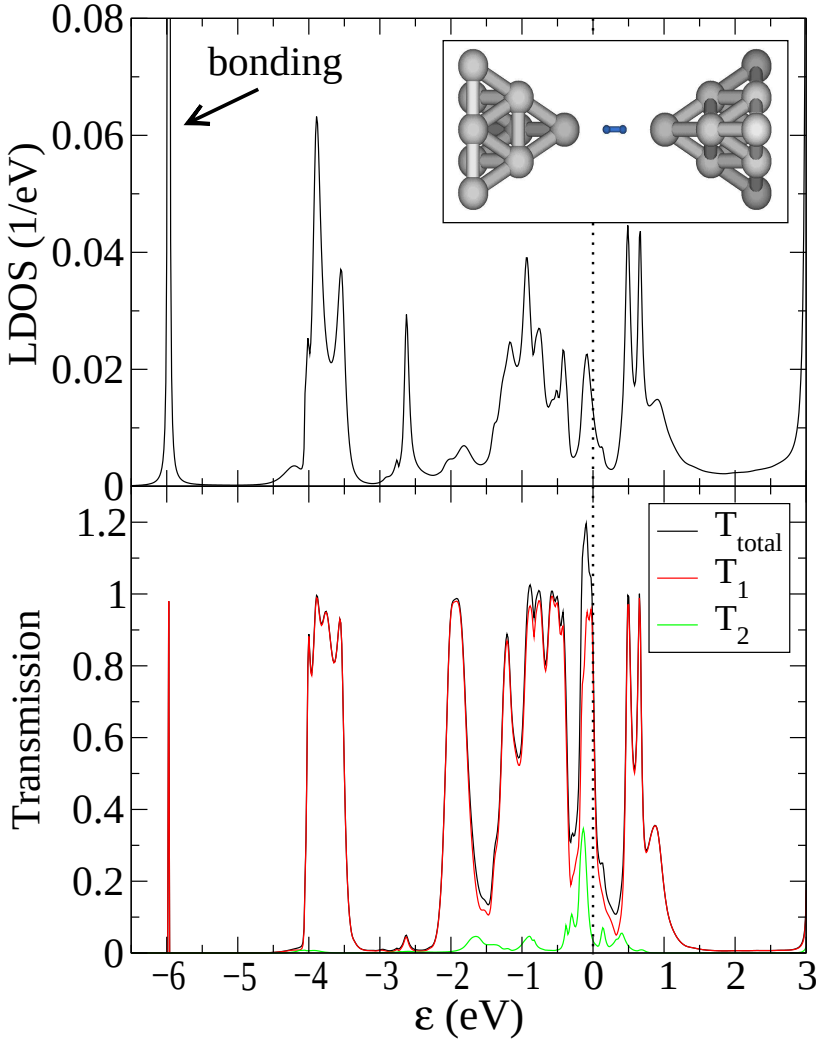

Figure 5. Transmission and LDOS projected into one of the H atoms as a function of energy for the Pt-H_2-Pt structure, the central cluster of which is shown in the inset. At E_F $T_1 = 0.83$ and $T_2 = 0.03$. The H-H and Pt-H distances are 0.8 Å and 2.1 Å respectively. We use the cc-pVDZ basis set for H.

each H is bound to three Pt atoms (hollow position). Indeed this configuration is suggested in studies of the chemisorption of H on Pt surfaces[29]. The conductance is carried by up to 7 individual channels (see Fig. 6). Due to the short distance between the Pt leads most of the current is bypassing the H_2 going directly from Pt to Pt. This analysis allows us to conclude that this type of geometries is not realized in the experiment and illustrates the importance of the channel analysis.

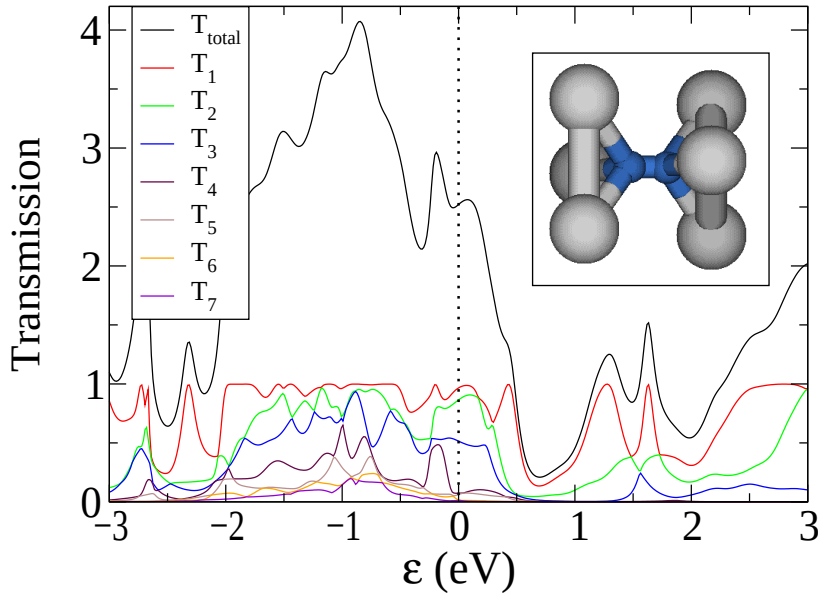

Figure 6. Transmission as a function of energy for the structure shown in the inset. The H-H and Pt-H distances are 0.8 Å and 1.86 Å respectively. The energy of the vibrational mode of the center of mass motion of H_2 is 65 meV.

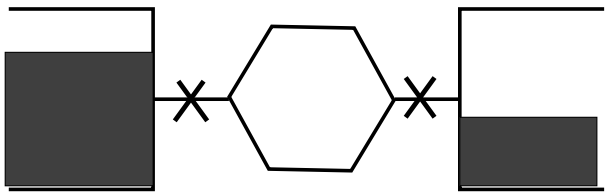

Figure 7. Schematic of the setup considered. A single benzene molecule is copuled at the para position via two tunnel couplings (X) to electrodes at the left and the right.

3 Weak Coupling

Using benzene as a prototypical example we investigate novel effects that arise when the molecule is weakly coupled to the electrodes (see Figure (7)) and transport through several competing electronic configurations becomes possible[18]. We derive a semi-quantitative model for the conducting many-body states of the system from electronic structure calculations. We compute the transport properties within the golden rule approximation (sequential tunneling) and include screening of the applied electric field as well as radiative transitions between the electronic states of the molecule. We predict a current collapse in the current-voltage characteristic and strong negative differential conductance (NDC) due to the occurrence of a "blocking" state when the molecule is coupled to the electrode at the para-position. For coupling at the meta-position, the current-voltage characteristic

displays a series of steps, but no NDC. We demonstrate how the specific *spatial* structure of the molecular orbitals qualitatively determines electronic transport. Finally, we discuss the limits of the model and the impact of disorder and symmetry breaking effects likely encountered in an experimental realization.

3.1 Model

To perform transport calculations in the weakly coupled regime, we extract an effective model from electronic structure calculations of the molecule. For benzene transport is assumed to be dominated by the π-electron system, but generalizations are straightforward. We first perform Hartree-Fock calculations in a suitable basis and then transform the Hamiltonian to the molecular orbital basis. We then integrate out the σ electrons of the system arriving at an effective *interacting* model Hamiltonian for the π electrons of the system in the presence of the atomic cores and the "frozen" density of the σ electrons:

$$\mathcal{H}_\pi = \sum_{ij\sigma} \epsilon_{ij} c^\dagger_{\sigma,i} c_{\sigma,j} + \sum_{ijkl\sigma\sigma'} U_{ijkl} c^\dagger_{\sigma,i} c^\dagger_{\sigma',j} c_{\sigma,k} c_{\sigma,l}. \tag{3}$$

The second quantized operators $c^\dagger_{\sigma,i}, c_{\sigma,i}$ create/destroy electrons of spin σ in orthogonalized Wannier-like orbitals centered at the carbon atoms. While this model neglects σ-π mixing for certain excited states of the molecule[30,31], its parameters account for the detailed electronic structure of the molecule. For the current work, we compute the model parameters only once, using an augmented double-zeta quality atomic natural orbital (ANO) basis set that was truncated to contain only one 2p-shell for each carbon. When applying a bias over the molecule this neglects the higher order effect of field screening by σ electrons and its impact on the π electrons.

We find that the low-energy spectrum of benzene obtained from the diagonalization of the effective Hamilton operator eq. 3 compares favorably with the spectrum directly obtained from accurate multi-reference configuration interaction calculations[31,32]. The remaining differences can be understood by the lack of σ-π mixing and do not qualitatively affect the transport properties. The restriction to a pure π-electron system is more severe for the charged states, as discussed in some detail below.

To account for the effect of an external bias potential V^{ext} on the electrons we include a term

$$\mathcal{H}_{bias} = e \sum_{ij\sigma\sigma'} V^{ext}_{ij} c^\dagger_{\sigma,i} c_{\sigma,j} \tag{4}$$

with $V^{ext}_{ij} = \int dr \Phi_i(r) V^{ext}(\hat{r}) \Phi_j(r)$ and $V^{ext}(\hat{r}) = (V_L + V_R)/2 - V_{bias}(\hat{r})$ in the Hamiltonian. $V_{L,R}$ is the chemical potential in the left/right electrode, distances are measured from the center of the molecule. The matrix elements V^{ext}_{ij} also result from the electronic structure calculation described above. We consider a bias $V_{bias} = V_L - V_R$ aligned with the transport direction (x-direction), unless otherwise specified.

To compute the transport properties of the system in the weak coupling limit we diagonalize the Hamiltonian eq. 3 in the appropriate charge, spin and symmetry sectors using a recently developed massively parallel implementation of the MRD-CI method[32,33]. Care is needed to handle degeneracies properly. After diagonalization of the Hamiltonian we have the many-body eigenstates $|s\rangle$ with the corresponding energies E_s and their total spin S_s.

We use a Master equation approach[17] for the occupation probabilities P_s in a stationary state. The transition rate $\Sigma_{ss'}$ from state s' to s is computed in perturbation theory using the golden rule. The "perturbation" is the coupling of the molecule to the leads

$$H_{mol-leads} = (\frac{\Gamma}{2\pi\rho_e})^{1/2} \sum_{\mathbf{k}\sigma\alpha l} \left(c^\dagger_{l\sigma} a_{\mathbf{k}\sigma\alpha} + h.c. \right) \ , \tag{5}$$

and (optionally) the coupling to electromagnetic fields (photons). Γ is the coupling strength (in units of energy) of leads to the benzene and ρ_e is the density of states of the electrons in the electrode (assumed constant). The operators $a_{\mathbf{k}\sigma\alpha}$ and their hermitian conjugates destroy/create electrons with momentum $\mathbf{k}$ and spin σ in electrode $\alpha =$ left/right For simplicity, we assume that tunneling is only possible through two "contact" carbon atoms which we choose to be at the 1 and 4 (para) positions unless noted otherwise.

As we do not consider the leads microscopically, the coupling of molecule states $|s\rangle$ is determined by the overall coupling strength Γ and the relative wave function amplitude of the state $|s\rangle$ at the coupling carbon site l. For the transition rates we have $\Sigma_{ss'} = (\sum_{\alpha,p=\pm} \Sigma^{\alpha p}_{ss'}) + \Sigma^d_{s,s'}$ where $\Sigma^{\alpha p}_{ss'}$ is the tunneling rate to/from electrode α for creation ($p = +$) or destruction ($p = -$) of an electron on the molecule.

The total transition matrix $\Sigma_{ss'}$ consists of blocks connecting N and $N \pm 1$ electron states (tunneling processes) and blocks from the radiative transitions that do not change the electron number on the molecule. Taking only one member of the subspace of spin and energy degenerate states into account, the rank r of the transition matrix is 1716. The stationarity condition $\dot{P}_s = 0$ can be written as $\sum_{s'} A_{ss'} P_{s'} = 0$ with the matrix $A_{ss'} = \Sigma_{ss'} - \sum_{s''} \Sigma_{s''s} \delta_{ss'}$. This implies that $A_{ss'}$ has an eigenvector with zero eigenvalue, which is the wanted solution for P_s. Rather than computing this eigenvector by brute force, to speed up the calculation we make use of $\sum_s P_s = 1$ to eliminate one row/column, thus reformulating the eigenvector problem into one of solving an inhomogeneous linear system of rank $r - 1$. Eventually, the current in the left and right electrode is calculated via

$$I_\alpha = e \sum_{s,s'} (\Sigma^{\alpha+}_{ss'} P_{s'} - \Sigma^{\alpha-}_{s's} P_s) \ . \tag{6}$$

3.2 Results

To elucidate the impact of various effects on the current we have performed transport calculations with and without radiative transitions (relaxation) and with and without effect of the applied bias. On the left panel of Fig. 8 we present the current-voltage characteristic obtained without the effect of the applied field (zero bias electronic structure). Without radiative relaxation (solid line) the current-voltage characteristic consists of a series of steps of which only a few are well resolved on this scale. The first step is associated with the population of the first π^* orbital of molecule (molecular charge $= -e$), an electron hops onto the lowest available level and then hops off again. At slightly larger bias, a transition of the anion to the first excited state of the neutral molecule becomes possible, resulting in a slight increase of the current. If the bias is sufficiently large this excited state may now accept another electron to populate higher excited states of the anion or low-lying states of the di-anion, resulting in a rapidly growing cascade of transitions between literally hundreds of states of the system. In the model considered here the growth of this cascade leads

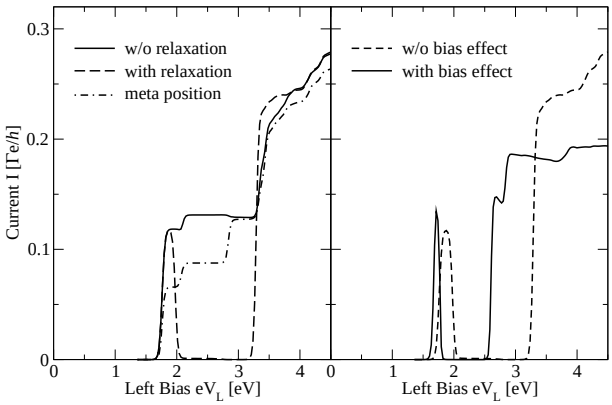

Figure 8. $I - V$ characteristics for symmetric bias. **Left Panel**: current-voltage characteristic without (solid line) and with radiative relaxation (dashed line) without inclusion of bias effect. The current collapses at a bias when the antisymmetric anion state can become occupied by radiative relaxation from an excited anion state. For coupling of the right electrode at the meta position (dash-dotted line) the radiative relaxation leads to no cascade into a blocking state and no current collapse is observed. **Right Panel**: With inclusion of the bias effect (solid line) the onset of current is generally shifted to lower bias, but the current collapse remains and additional weak NDC occurs at larger bias.

to quasi-ohmic behavior above 3.6 eV. In our calculation the first states of the di-anion become occupied at about 4.5 eV.

The inclusion of radiative transitions has a dramatic effect on the current-voltage characteristic (dashed line). We observe a collapse of the current over a substantial range of the applied bias (2.1-3.4 eV). The reason for this collapse is the population of a "blocking" state in the cascade of transitions that becomes possible when exited states of the neutral molecule and anion become accessible. Above approximately 2.1 eV bias an excited state of the anion at about 5.6 eV (see Fig. 9), becomes partially populated in the transport cascade. This state can decay by photon emission to either a symmetric or an antisymmetric many body state (with respect to the plane through the transport axis and perpendicular to the molecular plane) of the anion. In the bias range of the current collapse this state cannot

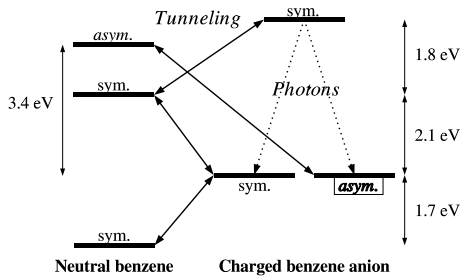

Figure 9. Sketch of the energetics and symmetry of the relevant neutral and anion states. At a left bias of 2.1 eV the antisymmetric blocking state becomes occupied via radiative relaxation. At 3.4 eV electrons can escape the blocking state via tunneling to the antisymmetric state of neutral benzene.

decay by coupling to the leads, because the lowest neutral states are symmetric (see Fig. 9) and the tunneling preserves the symmetry. Since there are no further radiative transitions possible on the molecule, the rate equations contain no draining term from this state. As a result, in the stationary state, the probability of occupying the "blocking" state is unity and the current ceases to flow. At a larger bias (3.4 eV), the first escape channel opens, and the system can decay to the first antisymmetric excited state of the neutral molecule, which can then decay further by photon emission.

The above calculations simplify the illustration of the mechanism of NDC, because the energies of the participating states are independent of the applied bias. In the physical system the various states couple differently to the applied field. The solid line in the right panel of Fig. 8 shows the current-voltage characteristic of the benzene with radiative relaxation and with the effect of the external potential applied parallel to the transport axis. We note a shift of the first step in the current-voltage characteristic , which is due to differential screening effects between the ground state of the neutral molecule and the anion. At larger bias, the differential effects on all of the states in the cascade result in a significant renormalization of the current-voltage characteristic . However, the current collapse still occurs, although the voltage window is reduced. The onset of quasi-ohmic behaviors occurs at higher voltage and a series of weak NDC effects occurs due to redistribution of occupation probabilities in favor of states with slightly smaller "transmission".

If we couple the right electrode to the meta position of benzene (left panel, dash-dotted curve) we find no current collapse with or without radiative relaxation or bias effect. This can be readily understood by the fact that at the meta position the wave function of the formerly blocking state is non-vanishing and electrons can tunnel out to the right electrode. Consequently, we observe a series of current steps similar (but not identical) to the case of coupling to the para position without relaxation.

4 Conclusions

We have presented an atomistic semi-quantitative description of non-linear transport through a single molecule junction. We were able to attribute distinctive features of the I-V of the symmetric and asymmetric molecule to their individual molecular levels obtained from *ab initio* calculations. The resolution of conductance into conduction channels permits a quantitative analysis of the contributions of individual orbitals to the overall transport. We have also presented a theory for the conductance of a hydrogen bridge between Pt contacts explaining the experimental observations. Furthermore we we able to describe transport in an idealized, though semi-quantitative, π-electron model of weakly coupled benzene and found a dramatic suppression of the current in a finite voltage window. In weakly coupled molecules the concept of the "blocking" state suggests new opportunities for the design of single molecule electronic devices.

These results were made possible through the use of large scale computational resources, such as those provided by the CRAY-T3E of the von Neumann Institute. In the strongly coupled limit it is advantageous to use as large electrode fragments as possible in the central cluster for which the DFT calculation is performed. For non-hybrid functionals the TURBOMOLE electronic structure program serves as a efficient, stable, parallel platform to carry out such calculations. In the weakly coupled limit, complex many-particle problems must be solved for all energetically relevant electronic levels of

the molecule. These calculations are performed with our massively parallel configuration selecting MRD-CI package. In both cases, these calculations should ideally be repeated for every applied voltage to account for charging effects. The required computational performance for such calculations presently requires the dedicated use of supercomputer facilities.

Acknowledgments

Regarding transport through the organic molecules we are grateful for many stimulating discussions with D. Beckmann, M. Mayor, H. Weber and F. Weigend. Regarding the transport through hydrogen we are grateful for many stimulating discussions with R.H.M. Smit, C. Untied and J.M. van Ruitenbeek. JCC acknowledges funding by the EU TMR Network on Dynamics of Nanostructures, and WW by the German National Science Foundation (We 1863/10-1), the BMBF and the von Neumann Institute.

References

1. M. C. Petty and M. R. Bryce, editors. *An Introduction to Molecular Electronics*. Oxford University Press, New York, 1995.
2. C. Joachim, J.K. Gimzewski, and A. Aviram. *Nature*, 408:541, 2000.
3. C. Joachim et. al. *PRL*, 74:2102, 1995.
4. S. Datta, W. Tian, S. Hong, R. Reifenberger, J. I. Henderson, and C. P. Kubiak. *Phys. Rev. Lett.*, 79:2530, 1997.
5. M. A. Reed, C. Zhou, C. J. Muller, T. P. Burgin, and J. M. Tour. *Science*, 278:252, 1997.
6. C. Kergueris, J.-P. Bourgoin, S. Palacin, D. Esteve, C. Urbina, M. Magoga, and C. Joachim. *PRB*, 59:12505, 1999.
7. D. Porath, A. Bezryadin, S. de Vries, and C. Dekker. *Nature*, 403:635, 2000.
8. J. Reichert, R. Ochs, D. Beckmann, H. B. Weber, M. Mayor, and H. v. Löhneysen. *Phys. Rev. Lett.*, 88:176804, 2002.
9. J. Chen, M. A. Reed, A. M. Rawlett, and J. M. Tour. *Science*, 286:1550, 1999.
10. U. Banin, Y. Cao, D. Katz, and O. Millo. *Nature*, 1999.
11. H. Park, J. Park, A. K. L. Lim, E. H. Anderson, A. P. Alivisatos, and P. L. McEuen. *Nature*, 407:52, 2000.
12. E. G. Emberly and G. Kirczenow. *Phys. Rev. B.*, 58:10911, 1998.
13. S. N. Yaliraki, A. E. Roitberg, C. Gonzalez, V. Mujica, and M.A. Ratner. *J. Chem. Phys.*, 111:6997–7002, 1998.
14. M. Di Ventra, S. T. Pantelides, and N. D. Lang. *Phys. Rev. Lett.*, 84:979, 2000.
15. J. Taylor, H. Guo, and J. Wang. *Phys. Rev.*, 63:121104R, 2001.
16. J. J. Palacios, et. al. *Phys. Rev.*, 64:115411, 2001.
17. M. Hettler, H. Schoeller, and W. Wenzel. *EPL*, 57:571, 2002.
18. M. Hettler M. Wegewis, H. Schoeller, and W. Wenzel. *Phys. Rev. Lett.*, 90:076805, 2003.
19. J. Park, A. Pasupathy, J. I. Goldsmith, C. Chang, Y. Yaish, J. R: Petta, M. Rinkoski, J.P. Sethna, H. D. Abruna, P. L. McEuen, and D. C. Ralph. *Nature*, 417, 2002.

20. W. Liang, M. P. Shores, M. Bockrath, J. R. Long, and H. Park. *Nature*, 417:725, 2002.
21. J. Heurich, J.-C. Cuevas, W. Wenzel, and G. Schoen. *Phys. Rev. Lett.*, 88:256803, 2002.
22. J. C. Cuevas, F. Pauly, J. Heurich, W. Wenzel, and G. Schön. Theoretical description of the electrical conduction in atomic and molecular junctions. *Nanotechnology*, (in press), 2003.
23. R. M. H. Smit, Y. Noat, C. Untiedt, N. D. Land and M.C. van Hermert, and J. M. van Ruitenbeck. *Nature*, 419:906, 2002.
24. J. C. Cuevas, A. Levy Yeyati, and A. Martín-Rodero. *Phys. Rev. Lett.*, 80:1066, 1998.
25. D. A. Papaconstantopoulos. *Handbook of the band structure of elemental solids*. Plenum Press, New York, 1986.
26. R. Landauer. *IBM J. Res. Develop.*, 1:223, 1957.
27. P. J. Hay and W. R. Wadt. *J. Chem. Phys.*, 82:299, 1985.
28. A. D. Becke. *J. Chem. Phys.*, 98:5648, 1993. B3LYP.
29. J. Kua and W .A. Goddard III. *J. Phys. Chem. B*, 102:9492, 1998.
30. B. O. Roos, K. Andersson, and M. P. Fülscher. *Chem.Phys.Letters*, 192:5, 1992.
31. T. Hashimoto, S. Nakano, and Hirao. *J. Chem. Phys.*, 104:6244, 1996.
32. P. Stampfußand H. Keiter and W. Wenzel. *J. Comput. Chem.*, 20:1559, 1999.
33. P. Stampfußand W. Wenzel. *Improved Implmentation and Application of the Individually Selecting Configuration Interaction Method*, pp. 215. Springer, 2002.